

Use of silver adatoms for the determination of the electrochemically active surface area of polycrystalline gold

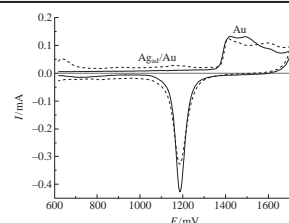
Yurii M. Maksimov and Boris I. Podlovchenko*

Department of Chemistry, M. V. Lomonosov Moscow State University, 119991 Moscow, Russian Federation.

Fax: +7 495 939 0171; e-mail: podlov@elch.chem.msu.ru

DOI: 10.1016/j.mencom.2017.01.020

Optimal conditions are found for estimating the electrochemically active surface area of polycrystalline gold based on a monolayer coverage with Ag_{ad} .



In fundamental studies on the behavior of catalysts for electrode reactions, the estimation of the electrochemically active surface area (EASA) (the term true surface was used earlier) is an important problem. For platinum-group metals, the EASA is usually determined by the adsorption of hydrogen, which cannot be applied to gold.^{1,2} Most frequently, the EASA of polycrystalline (pc) gold (both compact and disperse) is determined as a charge consumed in the adsorption/desorption of oxygen.^{1–6} The drawbacks of this method include the destruction of an Au surface layer due to the adsorption/desorption of O_{ads} and the noticeable Au dissolution during the repeated potential cycling of the Au electrode to high anodic potentials.^{6–8} The possibility of assessing the EASA of Au based on the monolayer of Cu adatoms (MLCu_{ad}) was mentioned.^{1,3,6} The adatoms of Ag are also candidates for the determination of the EASA of Au because Au and Ag have the same lattice type (face-centered cubic) and very close lattice parameters ($a = 0.4078$ nm for Au and 0.4086 nm for Ag). However, literature data on the formation of the Ag_{ad} layer at the potentials close to that of the Ag^+/Ag pair are very controversial: the assessed surface coverage with Ag_{ad} varies from $\sim 0.5^5$ to $\sim 1.0^{4,9,10}$ or $\sim 1.3^{11}$. It was of interest to study the behavior of Ag_{ad} on pc Au for estimating the EASA of Au based on MLAg_{ad} . The results are compared with the EASA values of the Au electrode determined based on Cu_{ad} .

Linear cyclic voltammetry (CVA) and coulometry, which consisted in the integration of CVA curves, were used. A three-electrode cell with separate anodic and cathodic compartments was employed. Unless otherwise specified, the working electrode potentials E were measured with respect to a reversible hydrogen electrode (RHE) in a supporting electrolyte solution of 0.5 M H_2SO_4 .¹² In $\text{Ag}_2\text{SO}_4 + 0.5$ M H_2SO_4 solutions on the silver electrode deposit, the equilibrium potentials of the Ag/Ag^+ pair vs. RHE (E_{Ag}) were measured for different Ag^+ concentrations, which allowed the potential scale of the reversible silver electrode to be used. These potential values are designated as E_{Ag}^{+0} ($E_{\text{Ag}}^{+0} = E - E_{\text{Ag}}$) and their positive values correspond to underpotentials that characterize the thermodynamics of Ag_{ad} .¹³

The gold plate electrodes were preliminarily cleaned by repeated potential cycling in 0.5 M H_2SO_4 at E from 0.050 to 1.9 V,⁶ after which E was cycled in a range of 0.090 – 1.70 V until the stationary CVA was established. Several electrodes with

different geometrical surfaces and roughness factors (from 2.5 to 3.5) were used. The surface areas determined through O_{ads} (EASA_0) were used as reference data for assessing the EASA values. The charge consumed in the electrodesorption of a monolayer of O_{ads} (MLO) was determined based on the anodic branch of a CVA measured in 0.5 M H_2SO_4 up to the potential of the current minimum (at $E \sim 1.65$ – 1.70 V).² The surface area was also calculated based on the relationship

$$\text{EASA}_0 = Q_0/400 \mu\text{C cm}^{-2}. \quad (1)$$

Figure 1 shows the CVA of an Au electrode in 0.5 M H_2SO_4 (curve 1) and 10^{-4} M $\text{Ag}_2\text{SO}_4 + 0.5$ M H_2SO_4 (curve 2). Curve 1 is typical of the pc Au electrode pretreated by potential cycling to 1.6 – 1.7 V.^{2,4,6} For this electrode, the EASA_0 was 3.3 cm² per cm² of the geometrical surface. Curve 2 was measured as we approached the potential $E_{\text{ads}} = 620$ mV in the cathodic run of CVA, for an Ag^+ adsorption time of 60 s. In special experiments, we found that an increase in the adsorption time did not induce noticeable changes in the adsorption value. The potential $E_{\text{ads}} = 620$ mV corresponds to $E_{\text{Ag}}^{+0} = 25$ mV. According to published data,^{5,10} the limiting gold surface coverage with Ag

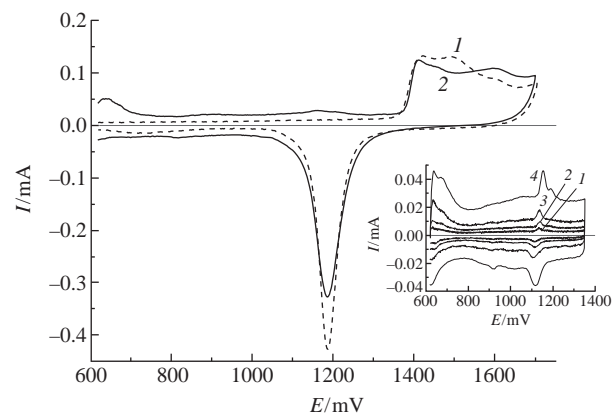


Figure 1 CVA on pc Au in the solutions of (1) 0.5 M H_2SO_4 and (2) 10^{-4} M $\text{Ag}_2\text{SO}_4 + 0.5$ M H_2SO_4 at $v = 20$ mV s⁻¹. Insert: CVA on pc Au in 10^{-4} M $\text{Ag}_2\text{SO}_4 + 0.5$ M H_2SO_4 solution at different v of (1) 5 , (2) 10 , (3) 20 and (4) 50 mV s⁻¹.

Table 1 Dependence of Q_{Ag} on v .

$v/\text{mV s}^{-1}$	$Q_{Ag}/\mu\text{C}$	$v/\text{mV s}^{-1}$	$Q_{Ag}/\mu\text{C}$	$v/\text{mV s}^{-1}$	$Q_{Ag}/\mu\text{C}$
1	413	10	414	50	397
5	410	20	410	100	386

adatoms at $C_{Ag^+} \leq 2 \times 10^{-4}$ M is reached at $E_{Ag^{+0}} \approx 50$ mV, *i.e.*, the chosen initial value of E_{ads} should be sufficient for the formation of $MLAg_{ad}$. The complete electrodesorption of Ag_{ad} occurs at $E_{Ag^{+0}} = 600\text{--}650$ mV.^{4,8,10} This allows one to remove Ag_{ad} at the potentials before the adsorption of O_{ads} on Au begins ($E > \sim 1.4$ V), which is very important for the accuracy and reproducibility of the determination of Q_{Ag} .

Figure 1 (insert) shows the CVA for the desorption/adsorption of Ag recorded at several potential scan rates v and $E = 0.62\text{--}1.34$ V. These CVA were recorded according to the following program: after the stationary CVA in 10^{-4} M $Ag_2SO_4 + 0.5$ M H_2SO_4 solution in the E range of $0.62\text{--}1.70$ V was attained, scanning in the cathodic direction was interrupted at $E = 620$ mV ($E_{Ag^{+0}} = 25$ mV) and this potential was maintained for 60 s, after which the linear potential scan was switched with the reversal at 1340 mV (without any delay at this value). This mode of measuring the CVA of adsorption/desorption of adatoms is designated below as mode I. Table 1 shows the values of Q_{Ag} obtained by integrating the anodic sections in CVA (mode I) recorded at different v , which were corrected for the charging of the electric double layer (EDL). Based on published data^{14–16} for gold, the average value of its double-layer capacitance (C_{EDL}) was taken to be $40 \mu\text{F cm}^{-2}$. Note that close C_{EDL} values are also known for Ag.¹⁷ This allowed us to disregard the fact that the surface under consideration was mixed (Ag–Au).

According to Table 1, for $v \leq 20$ mV s⁻¹, Q_{Ag} is almost independent of v . For $v > 20$ mV s⁻¹, a certain decrease in Q_{Ag} is observed being probably associated with the fact that small amounts of Ag_{ad} may desorb at potentials above the chosen anodic limit of CVA ($E = 1.34$ V).

Based on the average value of $Q_{Ag} = 412 \mu\text{C}$ (for $v \leq 20$ mV s⁻¹) at $Q_O = 970 \mu\text{C}$, we have found that the surface coverage with Ag_{ad} ($\theta_{Ag} = 2Q_{Ag}/Q_O$) in 10^{-4} M Ag_2SO_4 is ~ 0.85 . When the surface was assessed based on the relationship

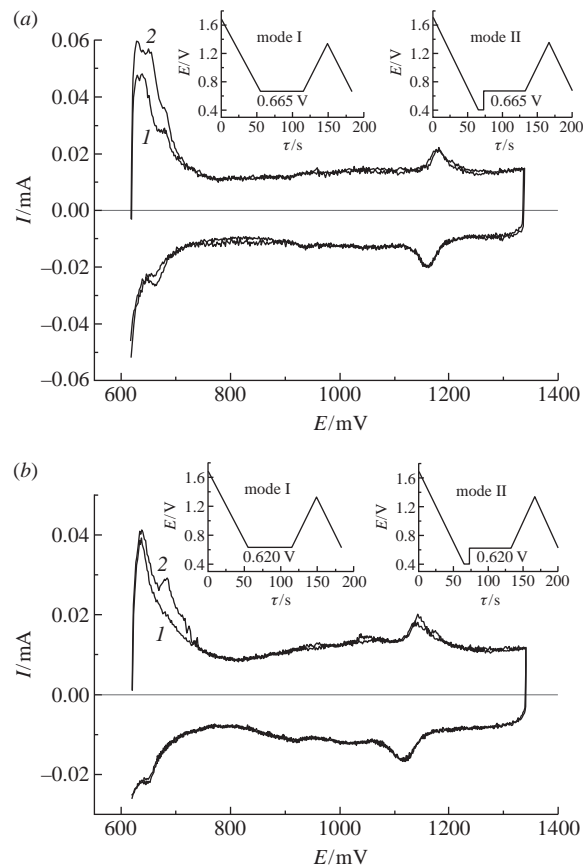
$$EASA_{Ag} = EASA_O \theta_{Ag}, \quad (2)$$

the obtained value was $\sim 15\%$ lower than $EASA_O$. In fact, using equation (2), we assume that $Q_{MLAg} = 0.5Q_{MLO}$, which means that variation of Q_{MLO} has no effect on the $EASA_{Ag}/EASA_O$ ratio equal to θ_{Ag} .

According to published data,^{5,9,18} at positive $E_{Ag^{+0}}$ close to 0, Ag adatoms form a poorly structured layer of nonstrict $Au_{surf}:Ag_{ad}$ stoichiometry. An indirect confirmation of the complicated nature of silver layer formation at high θ_{Ag} is a considerable difference in the shape and potential of the anodic and cathodic peaks in CVA at $E < 750$ mV (see insert in Figure 1). In this connection, one can expect the dependence of the surface stoichiometry on the Ag^+ concentration and conditions of $MLAg_{ad}$ formation.

Table 2 Found values of Q_O , Q_{Ag} , and Q_{Cu} and the corresponding values of EASA ($S_{geom} = 0.9 \text{ cm}^2$).

Entry	Solution	$Q_O/\mu\text{C}$	$EASA_O/\text{cm}^2$	$Q_{Ag}/\mu\text{C}$	θ_{Ag}	$EASA_{Ag}/\text{cm}^2$	$Q_{Cu}/\mu\text{C}$	θ_{Cu}	$EASA_{Cu}/\text{cm}^2$
1	10^{-3} M Ag_2SO_4 (mode I)	995 ± 20	2.49 ± 0.05	447 ± 15	0.90 ± 0.05	2.24 ± 0.17			
2	10^{-3} M Ag_2SO_4 (mode II)	995 ± 20	2.49 ± 0.05	477 ± 15	0.96 ± 0.05	2.39 ± 0.18			
3	10^{-4} M Ag_2SO_4 (mode I)	981 ± 20	2.45 ± 0.05	417 ± 15	0.85 ± 0.05	2.09 ± 0.17			
4	10^{-4} M Ag_2SO_4 (mode II)	981 ± 20	2.45 ± 0.05	436 ± 15	0.89 ± 0.05	2.19 ± 0.17			
5	2×10^{-3} M $CuSO_4$ (mode I)	987 ± 20	2.47 ± 0.05				701 ± 15	0.71 ± 0.03	1.75 ± 0.11
6	2×10^{-3} M $CuSO_4$ (mode II)	987 ± 20	2.47 ± 0.05				940 ± 20	0.95 ± 0.04	2.33 ± 0.14

**Figure 2** CVA on pc Au in the solutions of (a) 10^{-3} M $Ag_2SO_4 + 0.5$ M H_2SO_4 and (b) 10^{-4} M $Ag_2SO_4 + 0.5$ M H_2SO_4 for silver adsorption in modes (I) I and (2) II. $v = 20$ mV s⁻¹.

Experiments similar to those described above were also carried out in a 10^{-3} M Ag_2SO_4 solution (*i.e.*, 2×10^{-3} M Ag^+). Furthermore, in addition to mode I, we used another voltammetric mode of $MLAg$ formation (mode II): after the stationary CVA ($0.60\text{--}1.70$ V) in 10^{-3} M $Ag_2SO_4 + 0.5$ M H_2SO_4 solution was obtained, the cathodic scan was continued to $E = 400$ mV, *i.e.*, to the potentials of silver-phase deposition (in this solution, E_{Ag} is 640 mV); the electrode was maintained at this potential for 8 s, after that its potential was switched to $E = 665$ mV and stayed there in the potentiostatic mode for 60 s [Figure 2(a)]. It is evident that the use of mode II resulted in larger values of Q_{Ag} (Figure 2; Table 2, entries 1 and 2).

The values of θ_{Ag} were ~ 0.90 if the potentials $E < E_{Ag}$ were not reached during the formation of $MLAg_{ad}$ (mode I) and ~ 0.95 if $MLAg_{ad}$ was formed at $E_{Ag^{+0}} < 0$, which was followed by the removal of a silver phase (mode II). An increase in θ_{Ag} for mode II was also observed in 10^{-4} M Ag_2SO_4 [Figure 2(b); Table 2, entries 3 and 4). The $EASA_{Ag}$ values of pc Au found based on the electrodesorption of Ag_{ad} in sulfuric acid solutions with $C_{Ag} \geq 2 \times 10^{-3}$ M were consistent with the $EASA_O$ values (especially for mode II).

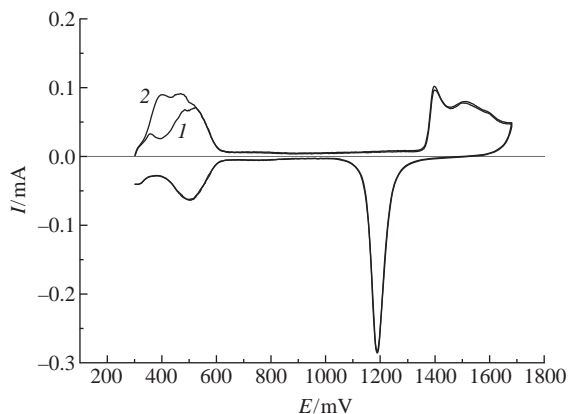


Figure 3 CVA on pc Au in the solution of 2×10^{-3} M $\text{CuSO}_4 + 0.5$ M H_2SO_4 upon the formation of MLCu_{ad} in modes (I) and (2) II. $v = 20$ mV s^{-1} . For explanations, see the text.

Table 2 shows the EASA_{Ag} values calculated based on equation (2). Insofar as we have assumed above that $Q_{\text{MLAg}} = 0.5Q_{\text{MLO}}$, the direct assessment of the surface on the basis of Q_{Ag} (without using EASA_{O}) should be carried out according to relationship $Q_{\text{Ag}}/200 \mu\text{C cm}^{-2}$. Such calculations led to the same EASA_{Ag} values but with a smaller standard deviation, e.g., we obtained $\text{EASA}_{\text{Ag}} = 477 \pm 15 \mu\text{C}/200 \mu\text{C cm}^{-2} = 2.39 \pm 0.075 \text{ cm}^2$ (see entry 2, Table 2).

At the same time, it was interesting to measure the gold-electrode EASA_{Cu} with respect to copper adatoms using two modes of MLCu_{ad} formation analogous to those used for Ag_{ad} . In mode I, MLCu_{ad} was accumulated at $E_{\text{ad}} = 300$ mV for 120 s (to obtain the stationary CVA, E was cycled in a range of 0.30–1.68 V). In mode II, the potential in the cathodic scan was brought to $E = 50$ mV ($E_{\text{Cu}^{2+}/0} \approx -190$ mV), maintained at this value for 6 s, switched to $E = 300$ mV ($E_{\text{Cu}^{2+}/0} = 20$ mV) for 120 s, after which the anodic scan was started. Figure 3 shows the corresponding CVA. As in the case of Ag_{ad} , upon the formation of MLCu_{ad} the higher Cu_{ad} coverages were obtained in mode II (this effect was even more pronounced). Difficulties associated with the formation of the well-structured MLCu_{ad} on gold with 1:1 stoichiometry were noted.¹⁹ The EASA_{Cu} values determined in mode II were in adequate agreement with the EASA_{O} values (Table 2).

The formation of adatomic layers of Ag and Cu depends to a large extent on the supporting-electrolyte anion.^{9,10,15} All estimates shown above pertain to sulfuric acid solutions and their applicability to other solutions requires a separate study. It can be assumed that the effect of sulfate and bisulfate anions manifests itself preferentially in their involvement in the EDL formation, whereas the anion adsorption values as such expressed in charge units do not exceed $10 \mu\text{C cm}^{-2}$ on pc Au.²⁰

Thus, the obtained results point to the possibility of assessing the EASA of pc Au by the electrodesorption of MLAg_{ad} . The

absence of strict $\text{Ag}_{\text{ad}}:\text{Au}_{\text{surface}}$ stoichiometry at underpotentials close to 0 imposes the more severe conditions on the MLAg_{ad} formation: the best results are obtained for $C_{\text{Ag}^+} \geq 2 \times 10^{-3}$ M and in the presence of a small amount of the Ag phase preliminarily deposited in the overpotential region. Meanwhile, attention should be drawn to the rather conditional character of the assumption that the AuO monolayer is present at $E = 1.6\text{--}1.8$ V because these potentials correspond to the mixed layer of various gold oxides.^{3,8,21} The satisfactory coincidence of the EASA values determined through metal adatoms with those determined through O_{ads} substantiates the correctness of the method put forward² for assessing the potential of pc Au at which oxygen is adsorbed in an amount equivalent to the O_{ads} monolayer.

References

- 1 S. Trasatti and O. A. Petrii, *J. Electroanal. Chem.*, 1992, **327**, 353.
- 2 A. A. Michri, A. G. Pshchenichnikov and R. K. Burstein, *Sov. Electrochem.*, 1972, **8**, 351 (*Elektrokhimiya*, 1972, **8**, 364).
- 3 R. Woods, in *Electroanalytical Chemistry*, ed. A. J. Bard, Marcel Dekker, New York, 1976, vol. 9.
- 4 S. Swathirajan, H. Mizota and S. Bruckenstein, *J. Phys. Chem.*, 1982, **86**, 2480.
- 5 M. C. Santos, L. H. Mascaro and S. A. S. Machado, *Electrochim. Acta*, 1998, **43**, 2263.
- 6 B. I. Podlovchenko, Ju. M. Maksimov and K. I. Maslakov, *Electrochim. Acta*, 2014, **130**, 351.
- 7 A. J. Rand and R. Woods, *J. Electroanal. Chem.*, 1972, **35**, 209.
- 8 C. L. Perdriel, A. J. Arvia and M. Ipohorski, *J. Electroanal. Chem.*, 1986, **215**, 317.
- 9 C. H. Chen, S. M. Vesceky and A. A. Gewirth, *J. Am. Chem. Soc.*, 1992, **114**, 451.
- 10 P. Mrozek, Y.-E. Sung, M. Han, M. Gamboa-Aldeco, A. Wiekowski, C.-H. Chen and A. A. Gewirth, *Electrochim. Acta*, 1995, **40**, 17.
- 11 K. Ogaki and K. Itaya, *Electrochim. Acta*, 1995, **40**, 1249.
- 12 B. I. Podlovchenko, T. D. Gladysheva and A. Yu. Filatov, *Mendelev Commun.*, 2015, **25**, 293.
- 13 D. M. Kolb, in *Advances in Electrochemistry and Electrochemical Engineering*, eds. H. Gerischer and C. W. Tobias, Wiley, New York, 1978, vol. 11, p. 125.
- 14 A. Hamelin, *J. Electroanal. Chem.*, 1986, **210**, 303.
- 15 A. Hamelin, *J. Electroanal. Chem.*, 1988, **255**, 281.
- 16 R. A. Manzhos, A. G. Krivenko, S. V. Doronin, M. A. Choba and V. A. Safonov, *J. Electroanal. Chem.*, 2013, **704**, 175.
- 17 V. A. Safonov, M. A. Choba, A. G. Krivenko, R. A. Manzhos and Yu. M. Maksimov, *Electrochim. Acta*, 2012, **61**, 140.
- 18 E. Herrero, L. J. Buller and H. D. Abruña, *Chem. Rev.*, 2001, **101**, 1897.
- 19 Y. Yu, Y. Hu, X. Liu, W. Deng and X. Wang, *Electrochim. Acta*, 2009, **54**, 3092.
- 20 G. Horanyi, E. M. Rizmayer and P. Joo, *J. Electroanal. Chem.*, 1983, **152**, 211.
- 21 K. Juodkazis, J. Juodkazyt, B. Šebeka and A. Lukinskas, *Electrochem. Commun.*, 1999, **1**, 315.

Received: 6th June 2016; Com. 16/4951